Alexander Schöch*, Patric Perez, Sabine Linz-Dittrich, Carlo Bach, and Carsten Ziolek

Automated surface inspection of small customer-specific optical elements

Automatische Oberflächeninspektion von kleinen benutzerspezifischen optischen Elementen

DOI 10.1515/teme-2017-0012
Received January 31, 2017; revised March 13, 2017; accepted March 28, 2017

Abstract: In industry, manual visual inspection is typically applied to assess surface imperfections on basic optical elements according to the standard DIN ISO 14997. This article proposes a machine vision setup to mimic the human tester's inspection process. It consists of multiple cameras and LED light sources. Both are arranged on the surface of a hemisphere with the optical element to be inspected at its center. By enabling individual LED sources on the hemisphere, any movement during acquisition can be omitted. Thus, the system is capable of acquiring a sparse pseudo BRDF (Bidirectional Reflectance Distribution Function) representation of imperfections. It is shown by experiments that this representation allows to discriminate between certain imperfections. Besides the mechanical setup, the image processing methodology and classification results are discussed. A comparison to results from manual inspection for 20 optical elements of the same geometry is also presented. Results indicate that a good agreement with the de-facto standard manual inspection method from industry can be obtained by the system.

Keywords: Quality control, automated surface inspection, optical elements, optical industry, BRDF.

Zusammenfassung: Oberflächenunvollkommenheiten an optischen Grundelementen werden typischerweise durch manuelle Sichtprüfung nach der Norm DIN ISO 14997 beurteilt. In diesem Artikel wird ein bildverarbeitendes System beschrieben, um den Inspektionsprozess eines menschlichen Testers nachzuahmen und zu automatisieren. Es besteht aus mehreren Kameras und LED-Lichtquellen, welche auf der Oberfläche einer Halbkugel angeordnet sind. Das zu untersuchende optische Element ist in der Mitte der Halbkugel platziert. Durch die Aktivierung einzelner LED-Quellen auf der Halbkugel kann jede Bewegung bei der Erfassung weggelassen werden. Somit ist das System in der Lage, eine dünnbesetzte pseudo-BRDF Repräsentation von Unvollkommenheiten in weniger als einer Sekunde zu erhalten. Neben dem mechanischen Aufbau werden die eingesetzten Bildverarbeitungsmethoden diskutiert. Es wird durch Experimente gezeigt, dass diese Darstellung erlaubt, zwischen bestimmten Arten von Unvollkommenheiten zu unterscheiden. Neben dem mechanischen Aufbau wird die Bildverarbeitung und Klassifikation von Defekten beschrieben. Ein Vergleich zu Resultaten der manuellen Inspektion für 20 optische Elemente derselben Geometrie zeigt gute Übereinstimmung mit der de-facto Standard-Inspektionsmethode aus der Industrie.

Schlüsselwörter: Qualitätskontrolle, automatische Oberflächeninspektion, Optische Elemente, Optische Industrie, BRDF.

***Corresponding author: Alexander Schöch,** Machine Vision Group, Institute for Production Metrology, Materials and Optics, NTB Interstate University of Applied Sciences of Technology Buchs, Werdenbergstrasse 4, 9471 Buchs, Switzerland,
e-mail: alexander.schoech@ntb.ch.
http://orcid.org/0000-0002-5245-0949
Patric Perez, Carlo Bach: Machine Vision Group, Institute for Production Metrology, Materials and Optics, NTB Interstate University of Applied Sciences of Technology Buchs, Werdenbergstrasse 4, 9471 Buchs, Switzerland
Sabine Linz-Dittrich, Carsten Ziolek: Technical Optics Group, Institute for Production Metrology, Materials and Optics, NTB Interstate University of Applied Sciences of Technology Buchs, Werdenbergstrasse 4, 9471 Buchs, Switzerland

1 Introduction

One aim of all manufacturing industries is to deliver defect-free products to their customers. This also applies for producers of basic optical elements where the production of e.g. lenses, mirrors or prisms becomes more

and more challenging due to continuously decreasing geometrical dimensions and tolerances, e.g. for application in medical devices. Moreover, customer specific requirements may result in small batch sizes. As a consequence, demands on quality control such as surface inspection are steadily increasing in terms of accuracy and flexibility. Even if surface imperfections may be solely of cosmetic interest [1–3], i.e. they do not significantly impair optical performance, customers often demand for high quality nevertheless.

Since surface inspection is nowadays typically done by human operators, more skilled personnel becomes necessary to retain quality. By the decreasing size of imperfections and varying customer-specific geometries, the time until fatigue may be reduced. Clearly, manual inspection is inevitably accompanied with variation in the results due to subjective perception [1–3]. Due to these shortcomings, several attempts for automated systems were made which are shortly reviewed in the next section.

2 Research context

A preceded survey by the authors indicates that quality control of basic optical components is typically done by means of manual visual inspection nowadays. During observation at six Swiss industrial optics manufacturers, it was ascertained that experienced testers detect and classify imperfections of lateral extensions down to 16 μm^2. They achieve such accuracy by use of various magnification utensils, a dedicated comparison artifact and proper variation of viewpoint and light source position w.r.t. the surface.

The definition of imperfections and test methods are addressed in the standards DIN ISO 10110-7 [4] and DIN ISO 14997 [5] respectively. Alternatively, an American MIL standard exists. The MIL-O-13830A uses a different approach and cannot be compared directly to the ISO counterpart [1]. This article is focused on testing methods regarding the ISO standard.

The DIN ISO 10110-7 defines a variety of different surface imperfections, such as: “Edge chips”, “Long scratches”, “Coating blemishes” and “Localized surface imperfections” which combine several regional defects and particles (orange boxes in Figure 1). These imperfections can be tolerated in technical drawings, what typically is written as follows:

$$5/N \times A; CN' \times A'; LN'' \times A''; EA'''$$

The “5” indicates the description of a surface imperfection tolerance. The four sections separated by a semicolon describe in order “Localized surface imperfections”, “Coating blemishes”, “Long scratches”, “Edge chips”. This enumeration corresponds to the orange boxes in Figure 1. The different N’s are the maximal number of occurrences of the respective imperfections. And the A’s represent an imperfections *grade*, defined by the maximal square root of its area in millimeters.

A dedicated mention of automated inspection systems is included in the draft version of the upcoming E DIN ISO 14997:2016-08 [6]. However, concerning automated systems, it does not assess boundaries or measurement guidelines. The main statement is a need of agreement between manufacturer and customer on a testing method.

Regarding automated systems, Turchette and Turner [3] propose a darkfield[1] microscope setup and image processing methods to specifically detect imperfections on laser resonator optics. They compare their results to manual visual inspection and cavity ringdown data and

1 Darkfield is a light setting where only scattered light is captured. Specular reflections are avoided by principle.

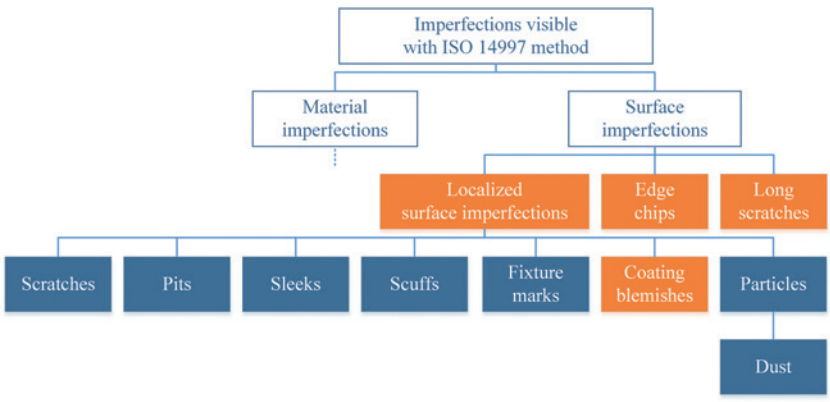

Figure 1: Classification of surface imperfections, based on DIN ISO 10110-7:2009-06 [4].

conclude a sufficient agreement. Clearly their method was applied on planar optics only, i.e. laser mirrors.

Liu et al. [7] propose a similar darkfield microscope setup and employ stitching techniques to achieve an expanded measurement area. They assess their results on photolithographic scratches and report errors about 3.5%. Experiments are again limited to planar optics.

To the knowledge of the authors, two commercial products to evaluate surface imperfections on optical elements are currently available.

The SavvyInspector [8, 9] from Savvy Optics Corp. employs a darkfield setup and a matrix sensor, allowing for a 1 mm × 1 mm inspection area. Besides its applicability for flat parts, also "mild concave" surfaces are advertised for. The system was originally designed to assess conformance to the American standard MIL-O-13830A but provides also an DIN ISO 10110-7 mode. For this, the minimal specified grade is $5/1 \times 0.025$ for a single imperfection and imperfection classes are limited to general defects and coating imperfections.

Recently, the Dioptic ARGOS system was presented [2]. It employs a line sensor and a rotation stage. A holistic representation of an optical element's surface is constructed by rotating the element during the acquisition phase and transforming the line sensor data accordingly. Their darkfield setup enables assessment of curved elements such as lenses by preliminary manual adjustment. It prevents the occurrence of specular reflections from curved surfaces and provides high resolution images up to 256 Megapixel. As minimal quantifiable grade, $5/1 \times 0.0025$ for single imperfections is stated and a repeatability between 0.4 µm and 1.3 µm based on 30 repetitions is reported. Etzold et al. [2] indicate that the system discriminates digs, scratches and edge chips.

The need for quality inspection of transparent parts is obviously not limited to classical optical components but also found in e.g. inspection of car headlamp lenses. Martinez et al. [10, 11] propose a dedicated lighting setup which is able to "move" a light source. By this method, a darkfield configuration is generated which yields sufficient image contrast during measurement.

It is worth noting that all reviewed approaches employ a darkfield setup and are mostly limited to planar optics. Neubecker and Hon [1] show that the signal contrast and the signal-to-background-noise ratio are potentially better than in brightfield conditions. However, they state that the direction of the maximal radiance, scattered by an imperfection, is almost unpredictable in a darkfield setup. This in turn could be accounted for by introducing movement of light sources and/or cameras or alternatively by multiple light sources and/or cameras. Neubecker and Hon [1] argue that mechanical actuators are slow and require more maintenance which is why a system capable to capture a sample with one shot is preferable.

3 Research goals

This work is a first step to advance current methods w.r.t.

1. Evaluation of camera positions and light scenario heuristics to enable holistic inspection on curved surfaces without mechanical movement.
2. Classification of different imperfection and particle types. In a first step, specification possibilities from the DIN ISO 10110-7 shall be covered (orange boxes in Figure 1). As further target, all of the imperfections indicated in Figure 1 shall be discriminated.

4 Acquisition system

As a starting point, first experiments were based on the manual inspection process which is in use at all surveyed optics manufacturers. This manual method of searching for imperfections is not trivial to reproduce in an automated system. A lot of movements, viewing angles and lighting conditions are based on inspector's experience. As expert knowledge grows, the operators can discriminate between imperfection categories and even link a defect to a manufacturing step.

However, the main light setting is a white light darkfield setting. First instincts lead to a diffuse light dome. This setup has already the potential to make a lot of typical defects visible and shows the main crux of the task: while it is feasible to find defects on a surface already in the field of view and in focus with appropriate light settings, it is, however, hard to detect imperfections on the whole curved surface of an optical component [1, 2].

4.1 Universal capture setup

In order to test for a multitude of camera poses and keep the experiments economically feasible, a surrogate dome was designed that allows to emulate different camera positions. As shown in Figure 2, the dome can be rotated around two orthogonal axes – this is equivalent to rotations of the camera around the dome's center and was preferred due to practical reasons. Clearly, camera positions are only feasible where the line of sight is not obstructed by the hemisphere's geometry, i.e. at the north pole and between strands.

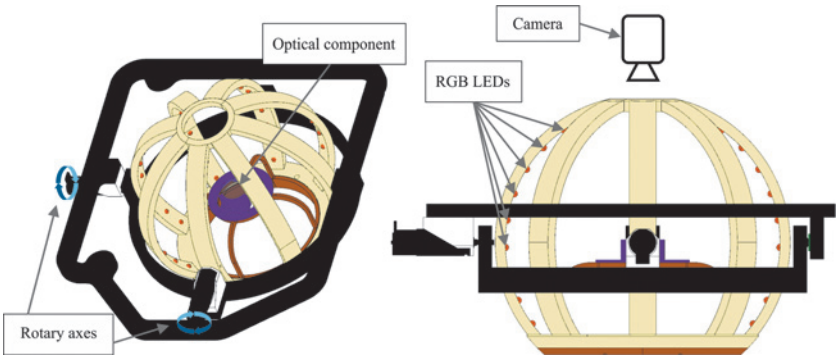

Figure 2: CAD drawing of the surrogate setup. RGB LED positions are indicated by orange spheres. Left: Isometric view. Right: Front view.

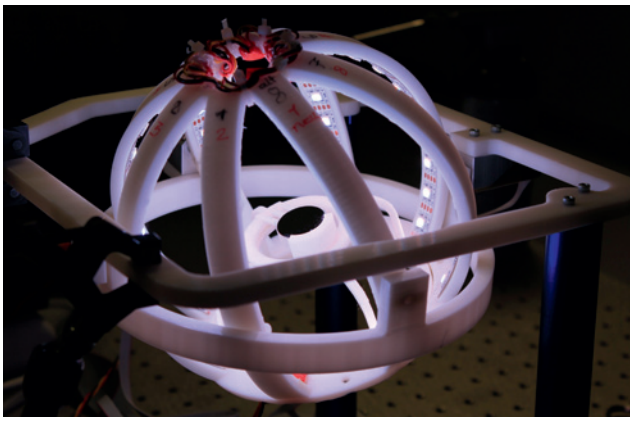

Figure 3: Photograph of the surrogate setup, slightly tilted with all LEDs enabled and a planar optical component inserted.

The dome consists of eight strands, with ten uniformly spaced LEDs attached to each of them (Figure 2). Each RGB LED can be controlled separately in intensity and color. This allows for discrete changes of the illumination angle, creating a brightfield or darkfield setting, as well as lighting scenarios with multiple sources enabled. To address the at times highly curved surface of convex or concave lenses, we needed to decide between either a multiple camera configuration or a rotation stage for our experimental setup. A rotation stage allows to look at each position on the sample surface with different angles and hence allows us to control the angle between illumination and camera-axis continuously. Regarding this correction possibility for the present surface normal, we decided for the rotation stage.

A major part of the dome was realized by means of additive manufacturing (Figure 3). The current setup uses a telecentric lens with a magnification ratio of 1 and a monochrome CCD camera.

4.2 First experiments

The described setup allows us to see all typical imperfections. To test the performance on small defects we made a comparison between some imperfection classes in our dome and a microscopy capture. With the current equipment we are able to detect defects down to a minimal grade of $5/1 \times 0.016$ for a single defect, as depicted in Figure 4.

A second typical and straightforward case is the scratch. It appears often as a set of digs or holes on a line. This example is shown in Figure 5. It is not significantly harder to find but a classification has to correctly link these single defects to a larger structure as they are evaluated as a whole scratch and not as single digs.

One of the imperfection types hard to image is the scuff. Scuffs are typically very small trenches with a continuous profile. They can be very small in width and vary extremely in length. One example is shown in Figure 6. Its width is about a micrometer but the length is more than two millimeters, it stretches over the whole convex lens. The images show a typical behaviour of those damages. They are only visible if illuminated from a very narrow sector of our dome. This explains the missing intersecting scuff from the microscopy image on the dome capture.

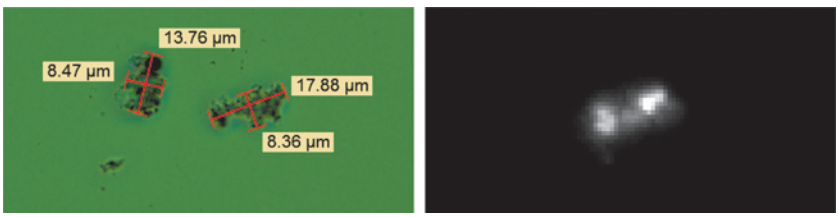

Figure 4: An example of a dig of size $5/1 \times 0.016$ on a planar mirror. On the left under a microscope and on the right with our dome.

Figure 5: This example shows a scratch with a width of about 5 µm. On the left under a microscope and on the right with our dome.

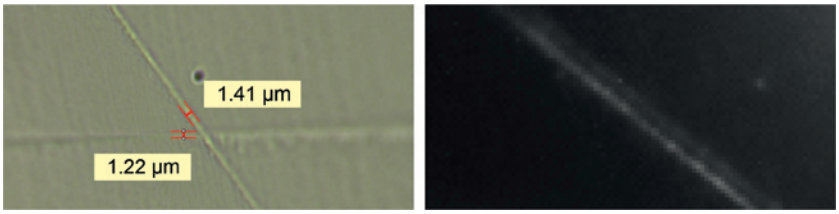

Figure 6: This is an example of our current limit. On the left a microscopy image where two scuffs can easily be seen. The horizontal scuff is only partly in focus because of the high curvature of the sample lens. The right image shows one of the scuffs under the dome with a single LED activated.

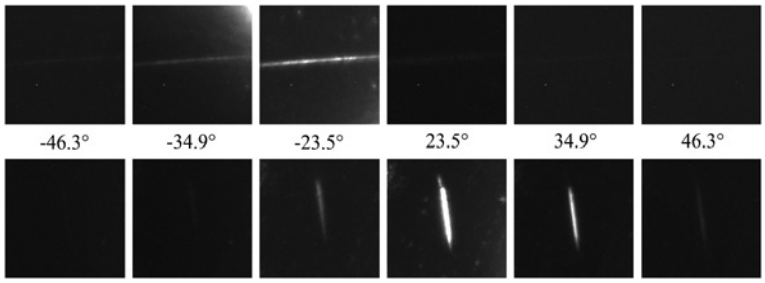

Figure 7: The two picture rows show different scuffs with a fixed camera position and changing light angle. Light is shining in a perpendicular azimuth angle to the scuffs axis but with changing polar angle as indicated.

From several examples and expert knowledge of the inspectors we know about some differences in appearance of different imperfection types. Some are quite hard to formulate quantitatively. But one particular rule is the visibility of scuffs. Experts describe the visibility of these as only a flashing if the illumination angle is perfect. This can easily be replicated. In the two image-collections in Figure 7 we visualise this behaviour. After testing multiple samples, we can express this by some rules. Scuffs are best visible if illuminated in a nearly brightfield condition, where the light source is preferably only tilted around the scuffs direction.

5 Image processing

Based on multiple images from different viewpoints and distinct lighting conditions, the position and grade of surface imperfections on the optical element is to be evaluated. The evaluation consists of preprocessing, specular reflex reduction, data fusion, segmentation and finally classification. These steps will be discussed in the following.

In order to constrain data processing to the optical element under consideration, a preprocessing step lets the user crop images and specify an appropriate mask, e.g. an ellipse. Note that these bounding box and mask parameters have to be requested only once per optical element geometry from the user.

Specular reflex reduction shall be discussed explicitly here, since it poses a non-trivial problem. On curved surfaces, specular reflexes from the involved LEDs are clearly visible in the images (Figure 8). The current approaches include (i) extraction and damping of circular reflexes without a priori knowledge; (ii) damping with a grayscale mask which consists only of the shape of reflexes, created by recording multiple elements of the same geometry and appropriate aggregation; (iii) creation of a grayscale mask as in (ii) but by knowledge of the setup and element geometry and means of raytracing; (iiii) simply reject images with reflexes. By several experiments, it was found that (ii) yields the best classification results if sufficient optical elements are used for the mask creation.

To obtain a holistic representation of the element's surface, the data from multiple viewpoints and lighting conditions is to be fused into a single dataset. A pair of viewpoint and lighting condition can be considered as one sensor. With such a definition, the utilised sensor configuration is complementary. Complementary configurations aim to combine information to give a more complete representation of a phenomenon and do not directly depend on each other [12].

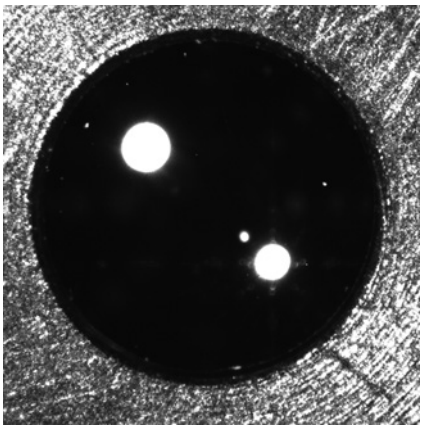

Figure 8: Example of specular reflexes on a lens with one LED enabled.

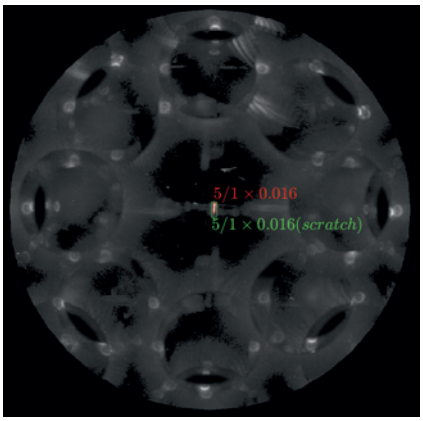

Figure 9: Example of a fused dataset from 48 lighting conditions and the classified defect at the center of the lens.

The applied approach fuses the datasets on pixel-level by a maximum criterion. For each pixel of all images from one viewpoint, the one with the highest intensity is chosen. Essentially, the resulting intensity a for one pixel at (x, y) for viewpoint index c is

$$a_{c,x,y} = \max\left(\{i_{c,l,x,y} \mid l \in [1..L]\}\right), \tag{1}$$

where L denotes the number of lighting configurations and $i_{c,l,x,y}$ is the intensity value of a pixel at (x, y) in an image taken from viewpoint index c with lighting configuration index l.

By this choice of aggregation, defects which result in relatively low intensities are retained. However, also specular reflexes would be kept what motivated the prior removal step. The aggregated dataset (example in Figure 10) is then used for segmentation of defects. Note that datasets from multiple viewpoints are not aggregated in the current setup and are instead processed separately.

As a first segmentation step, Bradleys method for adaptive thresholding [13] is applied. To combine the visibly separated but causally connected regions of a scratch, a mix of principal component analysis (PCA) and clustering is used. The angle and eccentricity, calculated from the PCA, and the position of defects span a 4D space which is used for clustering. Each dimension is multiplied by a factor to weight the involved features appropriately. Starting from the region with highest eccentricity, K-nearest neighbor clustering is performed. An example of clustering for a scratch is shown in Figure 9.

The last step classifies the extracted regions according to the DIN ISO 10110-7 and DIN ISO 14997 standards. First, the class of a defect is evaluated by its position and eccentricity, e.g. edge chips are connected to the border of the optical element and scratches have a higher eccentricity than digs. The grade is then determined by geometrical means, according to the previously evaluated class. However, not only the number of pixels and the magnification ratio is evaluated to assign a grade to a defect but also the pixel intensity. Since manual inspectors estimate the size of a defect mostly by the perceived brightness, the system also incorporates this information. Grades are rounded according to Annex E in DIN ISO 14997 [5]. An exemplary result of successful classification is given in Figure 10.

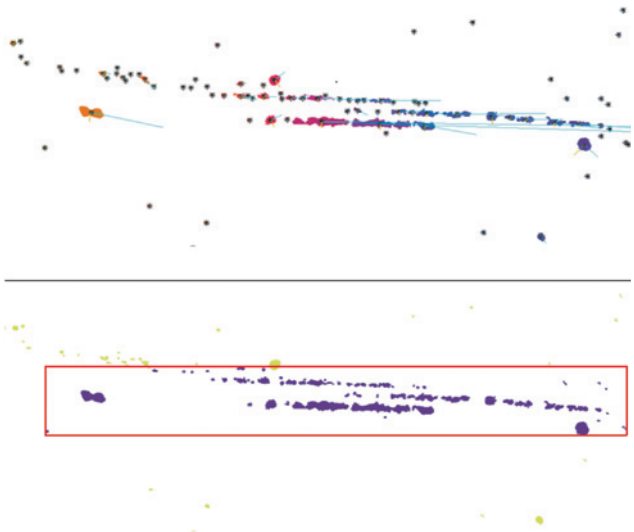

Figure 10: Regions of a scratch, colors indicate the region index. Top: Regions before merging. Bottom: Regions after merging by PCA and clustering, merged regions with the same index are indicated by a bounding box.

6 Comparison to manual visual inspection

By our project partners from industry we have access to large batches of optical elements of the same geometry. In addition, they do have inspection personnel to test these batches at an industrial grade. This allows us to do a larger scale testing of each different geometry with known and viable inspection results.

We generated our data basis with batches of different geometries. For each batch, the first step is a rigorous manual inspection by our partners according to the DIN ISO 14997 standard. They generate a protocol for each geometry where all found imperfection are documented in type, size and location. As a second step, the same elements are inspected by our system, keeping them as dust-free as possible in our non-cleanroom environment. In a last step, results are compared and visualized. This comparison is presented in the following for one batch.

6.1 Results

The batch consists of 20 biconvex lenses, having a total of 22 different defects on 16 of these lenses. Four lenses did not have any defect at all. Typically, we face the problem of particles or streaks (Figure 12). The presence of particles is caused by the non-cleanroom environment in our laboratory, streaks are mainly caused by the attempt to remove particles by manual cleaning. Thus, our evaluations naturally result in additional defects. As they are technically correct detections, they are caused by handling and were obviously not assessed by our industrial partners beforehand.

This usually results in a huge miscount error due to all the additional and only partially valid defect occurrences. To check our main objective, we started to assess the true-positives and false-negatives, as these results of real imperfections have a strong impact on our project viability.

Within this batch only one defect has not been detected by our dome setup. The single not detected defect was neither visible for humans in the acquired images. We suppose that the lack of sufficient lighting positions causes this invisibility. Additionally to the detection rate, the differences in the reported grade were evaluated and are given in Figure 11 that shows a histogram of the difference between automatic and manual detection. The results indicate that the system currently underestimates

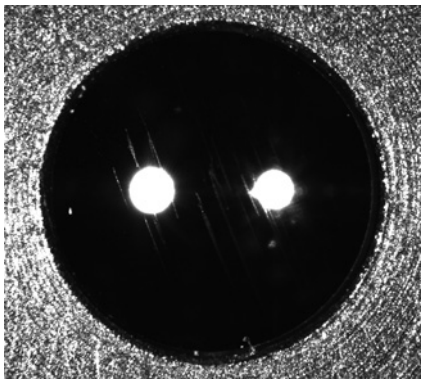

Figure 11: Camera image of a lens with dust particles and streaks.

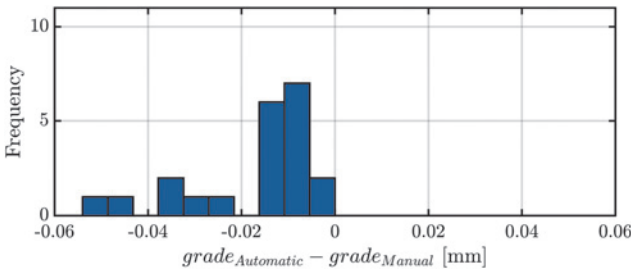

Figure 12: Defect grade classification performance for 20 biconcave lenses.

defect grades from manual inspection by maximally 60 µm, whereas 15 results deviated by less than 20 µm.

The manual and automatic inspection systems have different shortcomings, despite the closely related inspection approach. This means at least in some cases our automatic system outperforms the manual inspection. As our capture system was not intended to fully resolve structures smaller than 4 µm, it is still possible to identify defects within this magnitude of size. A good example are the scratches shown in Figure 13. The manual inspection found only the biggest vertical scratch, which is about 2 µm wide. Inspection by our system revealed additional differently oriented scratches, which we confirmed using microscope imaging. In other cases the manual approach is still superior, mostly where more flexibility or experience is required.

7 Conclusions

The current surrogate setup allows to mimic the manual inspection process according to the DIN ISO 14996 standard for surface imperfections in an automated way.

To discriminate between scuffs and other types of imperfections we capture a set of images with different LED settings and formulate a sparse pseudo BRDF. We call this

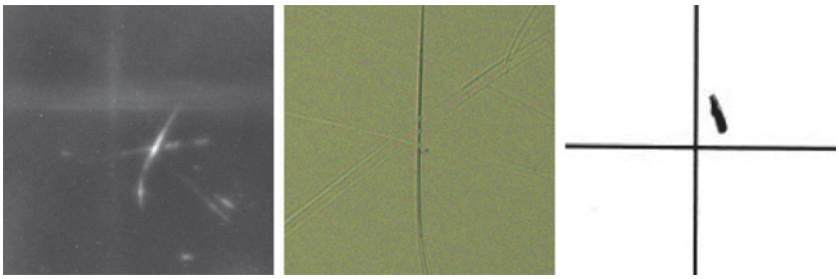

Figure 13: Three images of the same section from the center of an evaluated lens: On the left using our dome with all LEDs activated. In the center captured with a microscope. The right image represents the defect map created by a professional inspector.

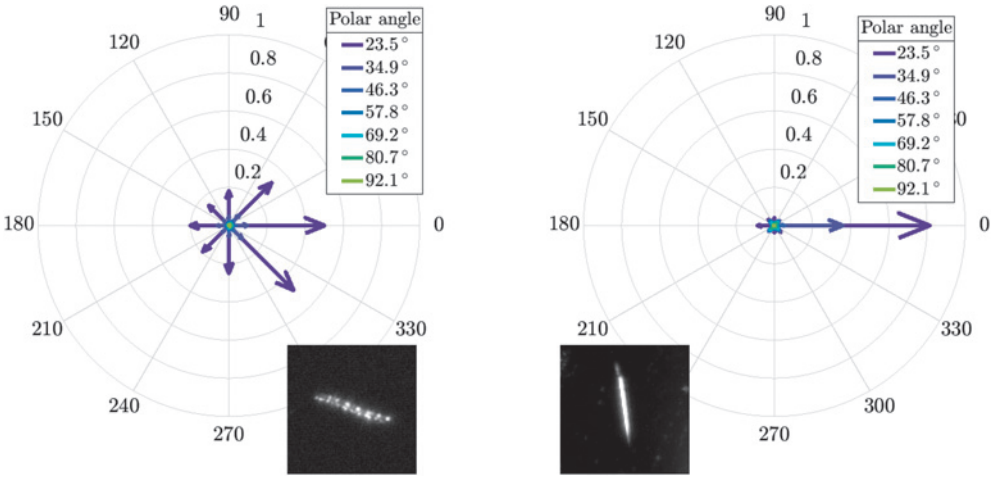

Figure 14: Comparison between a sparse pseudo BRDF of the scratch from Figure 5 (left) and the lower scuff from Figure 7 (right).

pseudo BRDF since the captured light intensity is evaluated and not the ratio between irradiance and reflected radiance. This, however, is sufficient because the aim is a relative comparison among defects.

As a prominent example, Figure 14 shows a scratch and a scuff with their correspondent pseudo BRDF evaluations. They seem similar in the visible area on the samples but have a significantly different reflection behaviour. Besides the given example, several experiments indicate that a pseudo BRDF representation of imperfections allows for discrimination between scuffs and scratches.

The current setup with its image processing software enables automatic detection and classification of defects according to the DIN ISO 10110-7 and DIN ISO 14997 standards. We demonstrated a detection rate of 21 out of 22 defects on a batch of 20 biconvex lenses.

8 Outlook

The gained understanding of most defect types under different illumination and camera angles leads to possible designs for a motionless setup. Essentially, mechanical motion shall be replaced by employing multiple cameras at appropriate positions. Moreover the need for a denser arrangement of lighting sources was identified during experiments and it is planned to be realized in the subsequent motionless setup.

One of the needs for classification is to find a possibility to discriminate between particles such as dust and surface imperfections. To achieve this, classification approaches such as from Li et al. [14] are to be tested with the system. Further promising possibilities to discriminate imperfections include the evaluation of the defect surfaces topography by means of multi view approaches [15].

Acknowledgement: The authors gratefully acknowledge the financial support by the Swiss state funding agency CTI (Commission for Technology and Innovation). This work was performed as project CTI 18084.1 “SurfInspect”: Automatic surface inspection of planar and spherical optical components.

References

1. Ralph Neubecker and Jenny E. Hon. Automatic inspection for surface imperfections: requirements, potentials and limits. In Rolf Rascher, Oliver Fähnle, Christine Wünsche, and Christian Schopf, editors, *Third European Seminar on Precision Optics Manufacturing*, SPIE Proceedings, page 1000907. SPIE, 2016.
2. Fabian Etzold, Daniel Kiefhaber, Arno F. Warken, Peter Würtz, Jenny Hon, and Jean-Michel Asfour. A novel approach towards

standardizing surface quality inspection. In Rolf Rascher, Oliver Fähnle, Christine Wünsche, and Christian Schopf, editors, *Third European Seminar on Precision Optics Manufacturing*, SPIE Proceedings, page 1000908. SPIE, 2016.
3. Quentin Turchette and Trey Turner. Developing a more useful surface quality metric for laser optics. In W. Andrew Clarkson, Norman Hodgson, and Ramesh Shori, editors, *SPIE LASE*, SPIE Proceedings, page 791213. SPIE, 2011.
4. DIN ISO 10110-7. Optics and photonics – Preparation of drawings for optical elements and systems – Part 7: Surface imperfection tolerances (ISO 10110-7:2008), 2009.
5. DIN ISO 14997. Optics and photonics – Test methods for surface imperfections of optical elements (ISO 14997:2011), 2013.
6. E DIN ISO 14997. Optics and photonics – Test methods for surface imperfections of optical elements (ISO/DIS 14997:2016), 2016.
7. Dong Liu, Yongying Yang, Lin Wang, Yongmo Zhuo, Chunhua Lu, Liming Yang, and Ruijie Li. Microscopic scattering imaging measurement and digital evaluation system of defects for fine optical surface. *Optics Communications*, 278(2):240–246, 2007.
8. David M. Aikens. The Truth About Scratch And Dig. In *Optical fabrication and testing: [part of] International Optical Design Conference and Optical fabrication and testing; 13–17 June 2010, Jackson Hole, Wyoming, United States*, OSA technical digest (CD). OSA, The Optical Society, 2010.
9. David M. Aikens. Objective Measurement of Scratch and Dig. In *Applied industrial optics: Spectroscopy, imaging and metrology; part of Imaging and applied optics; 24–28 June 2012, Monterey, California, United States*, OSA technical digest (online). OSA, The Optical Society, 2012.
10. S. Satorres Martínez, Gómez J. Ortega, Gámez J. García, and Sánchez A. García. A machine vision system for defect characterization on transparent parts with non-plane surfaces. *Machine Vision and Applications*, 23(1):1–13, 2012.
11. S. Satorres Martínez, J. Gómez Ortega, J. Gámez García, A. Sánchez García, and E. Estévez Estévez. An industrial vision system for surface quality inspection of transparent parts. *The International Journal of Advanced Manufacturing Technology*, 68(5–8):1123–1136, 2013.
12. Albert Weckenmann, X. Jiang, K.-D. Sommer, Ulrich Neuschaefer-Rube, Jörg Seewig, Laura Shaw, and T. Estler. Multisensor data fusion in dimensional metrology. *CIRP Annals – Manufacturing Technology*, 58(2):701–721, 2009.
13. Derek Bradley and Gerhard Roth. Adaptive Thresholding using the Integral Image. *Journal of Graphics Tools*, 12(2):13–21, 2011.
14. Lu Li, Dong Liu, Pin Cao, Shibin Xie, Yang Li, Yangjie Chen, and Yongying Yang. Automated discrimination between digs and dust particles on optical surfaces with dark-field scattering microscopy. *Applied Optics*, 53(23):5131–5140, 2014.
15. Richard Hartley and Andrew Zisserman. *Multiple view geometry in computer vision*. Cambridge University Press, Cambridge, UK and New York, 2nd edition, 2003.

Bionotes

Dr. Alexander Schöch
Machine Vision Group, Institute for Production Metrology, Materials and Optics, NTB Interstate University of Applied Sciences of Technology Buchs, Werdenbergstrasse 4, 9471 Buchs, Switzerland
alexander.schoech@ntb.ch

Dr. Alexander Schöch received his BSc in computer engineering and his MSc in industrial engineering from the NTB where he worked on cryptoanalysis with FPGAs and highly parallelized software frameworks respectively. He received his PhD degree from the University of Padua for his work on the topic of metrology at elevated temperature and industrial process control. Currently, he is employed as a research associate at the Institute for Production Metrology, Materials and Technical Optics (PWO) of NTB. His interests include computer graphics, computer vision and machine learning technology.

Patric Perez, B.Sc.
Machine Vision Group, Institute for Production Metrology, Materials and Optics, NTB Interstate University of Applied Sciences of Technology Buchs, Werdenbergstrasse 4, 9471 Buchs, Switzerland
patric.perez@ntb.ch

Patric Perez received a BSc in systems engineering with specialisation in computer engineering from the NTB. He created an interactive android teaching game for electrostatics and magnetism on bachelor level. Since his graduation he is employed at the Institute for Production Metrology, Materials and Technical Optics (PWO) of NTB as research associate. His main activities are planning and realisation of machine vision setups and subsequent image processing as applied research.

Dipl.-Phys. Sabine Linz-Dittrich
Technical Optics Group, Institute for Production Metrology, Materials and Optics, NTB Interstate University of Applied Sciences of Technology Buchs, Werdenbergstrasse 4, 9471 Buchs, Switzerland
sabine.linz@ntb.ch

Sabine Linz-Dittrich completed an apprenticeship as an optician at the company Zeiss in Jena. Afterwards she studied Optical Hardware and Spectroscopy Engineering at the institute LITMO in St. Petersburg, Russia. She completed her physics diploma thesis at the TU Berlin with the focus on thin film solar cells. During eleven years she was employed at Balzers Optics in Liechtenstein, there she gained experience as a development engineer in optical coatings as well as leading a production line of optical components. Since 2010 she is employed as a research associate at the Institute for Production Metrology, Materials and Technical Optics (PWO) of NTB.

Prof. Dr. Carlo Bach
Machine Vision Group, Institute for Production Metrology, Materials and Optics, NTB Interstate University of Applied Sciences of Technology Buchs, Werdenbergstrasse 4, 9471 Buchs, Switzerland
carlo.bach@ntb.ch

Prof. Dr. Carlo Bach received his diploma and his PhD in computer science from ETH Zurich. After several years in industry working in the field of artificial intelligence he joined the university of applied sciences NTB where he teaches computer science and image processing courses. Mr. Bach leads the machine vision group of the Institute for Production Metrology, Materials and Technical Optics (PWO). He is interested in all kinds of surface inspection with 2D and 3D methods.

Prof. Dr. Carsten Ziolek
Technical Optics Group, Institute for Production Metrology, Materials and Optics, NTB Interstate University of Applied Sciences of Technology Buchs, Werdenbergstrasse 4, 9471 Buchs, Switzerland
carsten.ziolek@ntb.ch

Carsten Ziolek finished his studies in physics at the University of Hanover in 1997 with a work on wavelength selection and Q-switching of erbium lasers. During his doctorate at the Laser Centre Hanover he worked on the laser dynamics of these systems. He earned his PhD in 2000 with a work on particular Erbium-based infrared-lasers for ophthalmology applications. From 2001 until 2015 he worked for the company TRUMPF in different positions, finally for more than 10 years as Head R&D of TRUMPF's marking lasers. In 2015 he was appointed as professor at the NTB. There he leads the Institute for Production Metrology, Materials and Optics as well as its technical optics and photonics field of competence. Carsten Ziolek is author of multiple technical publications and talks and is also involved in numerous patents.